Thermodynamic Characterization of the Osmolyte- and Ligand-Folded States of *Bacillus subtilis* Ribonuclease P Protein†

Christopher H. Henkels and Terrence G. Oas*

Department of Biochemistry, Box 3711, Duke University Medical Center, Durham, North Carolina 27710

Received March 11, 2005; Revised Manuscript Received June 27, 2005

ABSTRACT: In *Bacillus subtilis*, P protein is the noncatalytic component of ribonuclease P (RNase P) that is critical for achieving maximal nuclease activity under physiological conditions. P protein is predominantly unfolded (D) at neutral pH and low ionic strength; however, it folds upon the addition of sulfate anions (ligands) as well as the osmolyte trimethylamine *N*-oxide (TMAO) [Henkels, C. H., Kurz, J. C., Fierke, C. A., and Oas, T. G. (2001) *Biochemistry 40*, 2777−2789]. Since the molecular mechanisms that drive protein folding for these two solutes are different, CD thermal denaturation studies were employed to dissect the thermodynamics of protein unfolding from the two folded states. A global fit of the free-energy of TMAO-folded P protein versus [TMAO] and temperature yields T_S, ΔH_S, and ΔC_p of unfolding for the poorly populated, unliganded, folded state (N) in the absence of TMAO. These thermodynamic parameters were used in the fit of the data from the coupled unfolding/ligand dissociation reaction to obtain the sulfate dissociation constant (K_d) and the ΔH and ΔC_p of dissociation. These fits yielded a ΔC_p of protein unfolding of 826 ± 23 cal mol^{-1} K^{-1} and a ΔC_p of 1554 ± 29 cal mol^{-1} K^{-1} for the coupled unfolding and dissociation reaction ($NL_2 \rightarrow D + 2L$). The apparent stoichiometry of sulfate binding is two, so the ΔC_p increment of ligand dissociation is 363 ± 9 cal mol^{-1} K^{-1} per site. Because N and NL_2 appear to be structurally similar and therefore similarly solvated using standard biophysical analyses, we attribute a substantial portion of this ΔC_p increment to an increase in conformational heterogeneity coincident with the $NL_2 \rightarrow N + 2L$ transition.

A central dogma in protein science asserts that a unique, well-defined tertiary structure is essential for protein function (*1*). Although this tenet may hold for most proteins, an emerging class of proteins do not abide by this structure−function principle. This group is known as the "natively unfolded" or "intrinsically unstructured/disordered" protein (IUP)[1] family and consists of either full-length proteins or protein domains that do not maintain fixed, compact folded structures when analyzed by various biophysical techniques (for reviews, see refs *1*−*5*). The diversity of biological functions that IUPs carry out is large (*5*). However, they can be classified into five broad functional categories: entropic chains, effectors, scavengers, assemblers, and display sites (*3*). All of these functional classes, except entropic chains, require the presence of a binding partner to carry out their function. Furthermore, a concurrent disorder-to-order transition occurs for the majority of the IUPs upon binding their physiological target (*6*). IUPs therefore are exemplary of proteins whose thermodynamic balance between folded and unfolded conformations favors the unfolded state. Thus, the thermodynamic coupling of ligand binding to protein folding can be considered an extreme case of "induced fit" (*7*). One potential consequence of this thermodynamic linkage is the formation of unique interaction surfaces as the favorable binding free energy can overcome the unfavorable folding free energy to lead to complex formation (*3*, *6*).

In addition to the formation of complementary surfaces with marginal stability, other possible functional advantages for IUPs have been advanced. These include (i) the regulation of cellular activity via targeted proteolytic degradation (*1*); (ii) the control of macromolecular assembly (*8*); (iii) the creation of extensive interaction surfaces that cannot otherwise be obtained with a compact protein (*3*); (iv) the potential to bind targets with a faster association rate (*9*); and (v) the ability to bind multiple ligands due to the inherent structural plasticity of the intrinsically disordered protein (*10*). Although speculative in nature, there are some intriguing thermodynamic implications of these putative IUP functions. For example, structural adaptivity of the poorly populated folded conformations of an IUP implies extensive structural heterogeneity in this thermodynamically unfavored folded ensemble. Certain ligands and/or stabilizing solutes

† Supported by National Institutes of Health grants GM45322 (T.G.O.). C.H.H. was supported in part by NIH Training Grant GM08487.

* To whom correspondence should be addressed. Tel: (919) 684-4363. Fax: (919) 681-8862. E-mail: oas@biochem.duke.edu.

[1] Abbreviations: CD, circular dichroism; C_{HS}, concentration at zero enthalpy and entropy; DSC, differential scanning calorimetry; GuanHCl, guanidinium hydrochloride; HSQC, heteronuclear single quantum coherence; IUP, intrinsically unstructured protein; L or lig, ligand; p21, p21-activated kinase; PFG-NMR, pulsed-field gradient nuclear magnetic resonance; per, perturbant; pI, isoelectric point; P protein, protein subunit of *Bacillus subtilis* ribonuclease P; pre-tRNA, precursor tRNA; RNase P, ribonuclease P; T_o, reference temperature; T_{HS}, temperature at zero enthalpy or entropy; TMAO, trimethylamine *N*-oxide; WASP, Wiskott−Aldrich syndrome protein.

10.1021/bi0504613 CCC: $30.25
Published on Web 09/02/2005

can specifically select particular folded conformations out of this ensemble. Indeed, this situation has been observed for IUP domains of the signaling proteins WASP and p21 (*11*) where the observed folded structure is ligand context-dependent.

One RNA-binding IUP that undergoes substantial disorder-to-order folding transitions upon the addition of various solutes is the ribonuclease P protein from *Bacillus subtilis* (P protein). P protein is the noncatalytic, highly basic protein that is associated with the ribozyme P RNA to form ribonuclease P (RNase P). RNase P is the ubiquitous endoribonuclease responsible for the 5′ maturation of precursor-tRNA (pre-tRNA) transcripts (for review, see refs *12*, *13*). Although P protein does not contain the catalytic components of RNase P, it is essential for in vivo catalysis (*14*). Furthermore, P protein has been shown to stabilize P RNA structure (*15*−*17*), modulate substrate specificity (*18*), and enhance the affinity of magnesium ions required for catalysis (*19*). P protein also enhances RNase P holoenzyme catalytic efficiency through the direct interaction of the protein with the 5′-leader sequence of pre-tRNA (*20*−*22*).

Previously, we showed that intrinsically unstructured P protein can be induced to refold in the presence of two different solvent additives: the osmolyte trimethylamine *N*-oxide (TMAO) and small molecule ligands such as sulfate anions (*23*). The principal driving forces for this folding transition are different for the two solutes. TMAO induces P protein folding through the "osmophobic" effect (*24*) arising from an unfavorable interaction between TMAO and the peptide backbone. In contrast, in sulfate, binding-competent conformers are selectively stabilized through ligand binding. Thus, the two types of perturbant may or may not populate the same P protein folded state. A principal motivation of this study is to determine whether there are appreciable differences in the thermodynamic properties of P protein refolded by addition of osmolyte or ligand. In particular, heat capacity differences are of interest because they have been used in the past to detect structural differences in biopolymer reactions.

The change in heat capacity, ΔC_p, for protein unfolding has been empirically correlated with the change in the solvent accessible surface area, ΔASA, between the unfolded and the folded conformations (for review, see refs *25*, *26*). The primary origin of ΔC_p for reactions in aqueous solution has been attributed to the difference in the extent of surface hydration between reactants and products (*27*). Moreover, polar and apolar surface exposure to solvent contribute in opposite manners to ΔC_p; increases in apolar surface exposure (ΔASA_{ap}) result in positive contributions to ΔC_p, while increases in polar surface exposure (ΔASA_{pol}) cause ΔC_p to be negative. These contributions are empirically additive with ΔASA so that ΔC_p has the form

$$\Delta C_p = C_{ap} \cdot \Delta ASA_{ap} + C_{pol} \cdot \Delta ASA_{pol} \qquad (1)$$

$C_{ap,pol}$ are the constants relating apolar and polar surface to heat capacity. C_{ap} and C_{pol} have been parametrized through the correlation between experimentally determined ΔC_p for protein unfolding and the predicted ΔASA from crystal and NMR structures and various models for the denatured state (*28*, *29*). Therefore, the hydration contributions to ΔC_p of any protein whose structure is known can be predicted (*27*). Although these predictions are cast in terms of solvation, nonsolvation contributions to ΔC_p are known to exist (*27*, *30*) and may be implicit in C_{ap} and C_{pol}.

Given that sulfate and TMAO drive P protein refolding by different molecular mechanisms, a thermodynamic study was undertaken to determine the ΔC_p of the folding transitions induced by the two stabilizing perturbants. Since preliminary biophysical data suggest that the two folded states are similar (*23*), the prediction is that the apparent ΔC_p for the two unfolding reactions would be identical or within error. Alternatively, any difference in apparent ΔC_p for forming the two folded states could imply conformational alterations between the ligand-folded and the osmolyte-folded states of P protein. Here, we use CD thermal denaturation studies of P protein in the presence of stabilizing solute (osmolyte or ligand) to obtain a thermodynamic description of temperature-induced unfolding of the ligand-folded and the TMAO-folded conformations of P protein, and thereby the ΔC_p of the two reactions.

EXPERIMENTAL PROCEDURES

Expression and Purification of P Protein. Recombinant *B. subtillis* RNase P protein was purified as previously described (*23*). Protein purity was determined to be >95% by SDS−PAGE analysis and by analytical HPLC analysis. The Edelhoch method as modified by Pace and Schmid (Protocol 1 in ref *31*) was used to calculate P protein stock concentrations. Molar extinction coefficients of 5800, 5600, 5120, and 4800 M^{-1} cm^{-1} were used at 276, 278, 280, and 282 nm, respectively.

Protein Sample Preparation. Concentrated protein solutions were prepared by dissolving the lyophilized protein into standard buffer (10 mM sodium cacodylate, pH 7). The protein stock solutions were then placed in a 37 °C water bath for at least 15 min followed by centrifugation at 15 000 rpm for 5 min to pellet any undissolved protein. Edelhoch measurements were subsequently used to determine the protein stock concentration.

To minimize the effect of pipetting error on protein concentration, P protein was diluted into two perturbant (e.g., sulfate or TMAO) stocks in standard buffer, one without perturbant (stock A) and one with a high concentration of perturbant (stock B). The protein concentration in the two perturbant stocks was 10 μM. The pH of stocks A and B were then adjusted to pH 7 accordingly using either NaOH or cacodylic acid. Special care was taken to ensure that the total amount of cacodylate added never exceed 50 mM, particularly in the high TMAO stock buffer, as the cacodylate anion can affect P protein stability above this concentration (data not shown). In all cases, the change in protein concentration due to addition of acid or base was <0.5%. Protein samples containing intermediate concentrations of perturbant were prepared by mixing the appropriate volumes of stocks A and B; the final volume of these samples was 3 mL. For the ligand denaturation surface, stock B contained 10 mM SO_4 and the series of intermediate sulfate concentrations were 0.05, 0.1, 0.2, 0.3, 0.4, 0.5, 0.6, 0.7, 0.8, 0.9, 1.0, 2.0, and 5.0 mM. The high osmolyte stock concentration was 2.12 M TMAO with intermediate sample concentrations of

0.10, 0.22, 0.32, 0.44, 0.56, 0.66, 0.72, 0.83, 0.91, 1.15, 1.24, and 1.44 M TMAO. The TMAO concentration was measured using refractive index as described by Bolen and co-workers (*32*). All samples were thoroughly degassed under vacuum prior to the experiment.

Circular Dichroism (CD) Spectroscopy. Far-UV circular dichroism measurements were carried out on an Aviv model 202 CD spectrophotometer equipped with a stirred thermoelectric cell holder. The CD signal at 222 nm was followed over a temperature range from 0 to 90 °C at 1 °C increments. The protein samples (2.5 mL) were placed in a 1 cm path length quartz cuvette and allowed to equilibrate at 0 °C for at least 20 min prior to denaturation. Previous experiments have shown that temperature equilibration occurs within this waiting period (*23*). An equilibration time of 30 s and a signal averaging time of 30 s were used during the thermal denaturation; the bandwidth was 1 nm, and a temperature dead band of 0.1 °C was used. A typical thermal denaturation takes around 3 h and was previously found to be 90−95% reversible under these experimental conditions (*23*). However, some protein aggregation was observed at elevated temperatures (>80 °C) in the presence of the high amounts of TMAO (>1.3 M) (C.H.H., unpublished results).

Thermal denaturations of various buffer controls were also performed to account for any temperature dependence in the CD signal of the cuvette, standard buffer, sulfate, and/or TMAO. Replicate denaturations of standard buffer alone at various times throughout the surface data collection showed very little signal change. Thermal denaturations of standard buffer with 20 mM Na_2SO_4 overlapped with the standard buffer alone, so the CD signal from each sulfate-containing protein sample was buffer-corrected with the standard buffer blank signal. There was a slight deviation observed between the CD signals arising from the thermal blanks of buffer containing 1 M TMAO and that of standard buffer (0 M TMAO) alone. Thus, the average signal from the 0 M TMAO and the 1 M TMAO thermal blanks was used to buffer-correct the CD signal from osmolyte-containing protein thermal denaturations. The final buffer-corrected CD signal at 222 nm was converted into mean residue ellipticity ($[\Theta]_{222}$).

Conversion of CD Signal to Fraction Denatured, $F_{d,exp}$, and Standard Gibbs Free Energy of Denaturation, ΔG_{exp}. The observed protein CD signal ($[\Theta]_{222}$) at any given temperature and perturbant concentration can be converted into the fraction of denatured protein, $F_{d,exp}(T,[per])$, using the following equation which is based upon the two-state assumption:

$$F_{d,exp}(T,[per]) = \frac{[\Theta]_{222} - B_N(T,[per])}{B_D(T,[per]) - B_N(T,[per])} \quad (2)$$

where $B_{N,D}(T,[per])$ are the signals arising from the temperature- and osmolyte-dependent native and denatured base surfaces, respectively. Results indicate that the native base surface is well-modeled as a simple baseplane (a three-parameter equation), while the denatured base surface required an additional cross term (a four-parameter equation) to describe its coupled temperature and perturbant dependencies (see below). Another assumption in eq 2 is that the CD signal arising from a native ensemble is the same regardless of liganded state (i.e., N, NL^{α}, NL^{β}, and NL_2). The fraction denatured data in the transition region, $0.05 < F_{d,exp}(T,[per]) < 0.95$, was further transformed into standard free energy of denaturation, $\Delta G_{exp}(T,[per])$, using the equations below

$$\Delta G_{exp}(T,[per]) = -RT \ln K_{eq}(T,[per]) \quad (3)$$

$$K_{eq}(T,[per]) = \frac{F_{d,exp}(T,[per])}{(1 - F_{d,exp}(T,[per]))} \quad (4)$$

$K_{eq}(T,[per])$ is the equilibrium constant of unfolding at any T and [per].

RESULTS

The Effect of Osmolyte and Ligand on the Thermal Denaturation of RNase P Protein. The goal of this study was to elucidate the thermodynamic mechanism by which the solutes TMAO (osmolyte) and sulfate (ligand) stabilize RNase P protein. To this end, thermal denaturation experiments (denaturations) were carried out in the presence of varying amounts of each solute (0−1.5 M TMAO or 0−10 mM sulfate) as monitored by CD at 222 nm ($[\Theta]_{222}$). The thermal denaturations of P protein in the presence of increasing amounts of TMAO and sulfate are shown in Figure 1, panels A and B, respectively. At [TMAO] > 0.22 M or $[SO_4]$ > 0.05 mM, there is a cooperative transition leading to a sigmoidal decrease in the observed $[\Theta]_{222}$ at elevated temperatures due to the loss of secondary structure on thermal unfolding. Increasing concentrations of either solute (molar for TMAO, and millimolar for sulfate) shift this transition to higher temperatures (Figure 1). Therefore, TMAO or sulfate act to stabilize P protein against thermal unfolding. Furthermore, at any temperature below 50 °C, the addition of progressively higher concentrations of either solute produces an isothermal sigmoidal transition to stronger $[\Theta]_{222}$ (Figure 1). This transition is due to the induced folding that occurs for the intrinsically disordered P protein upon the addition of either osmolyte or ligand (*23*).

At low perturbant concentrations (0−0.22 M for TMAO and 0−0.05 mM sulfate), a slight increase in $[\Theta]_{222}$ (to more negative) is observed at extremely low temperatures (Figure 1). This downward curvature at low temperatures is not well-fit to the linear unfolded baseline model used in this study (eq 5, see below) and may be due to the formation of an additional conformation of P protein that is favored at extremely low temperatures (<0 °C). The deviation from linearity does not occur in the 10−20 °C range where the intermediate thermal denaturations reveal a CD signal minima (Figure 1), which is likely to be near the temperature of maximum stability for P protein. Therefore, the data at low temperatures and very low perturbant are not included in the surface analysis.

In the analysis described here, the surfaces depicted in Figure 1 are subjected to nonlinear least-squares analysis in two steps. First, the data points corresponding to fully folded and unfolded protein are selected by inspection to define the completely folded and unfolded base surfaces. These data points ultimately determine the $[\Theta]_{222}$ of the folded and unfolded states at all temperatures and perturbant concentrations: $B_N(T,[per])$ and $B_D(T,[per])$, respectively. The data

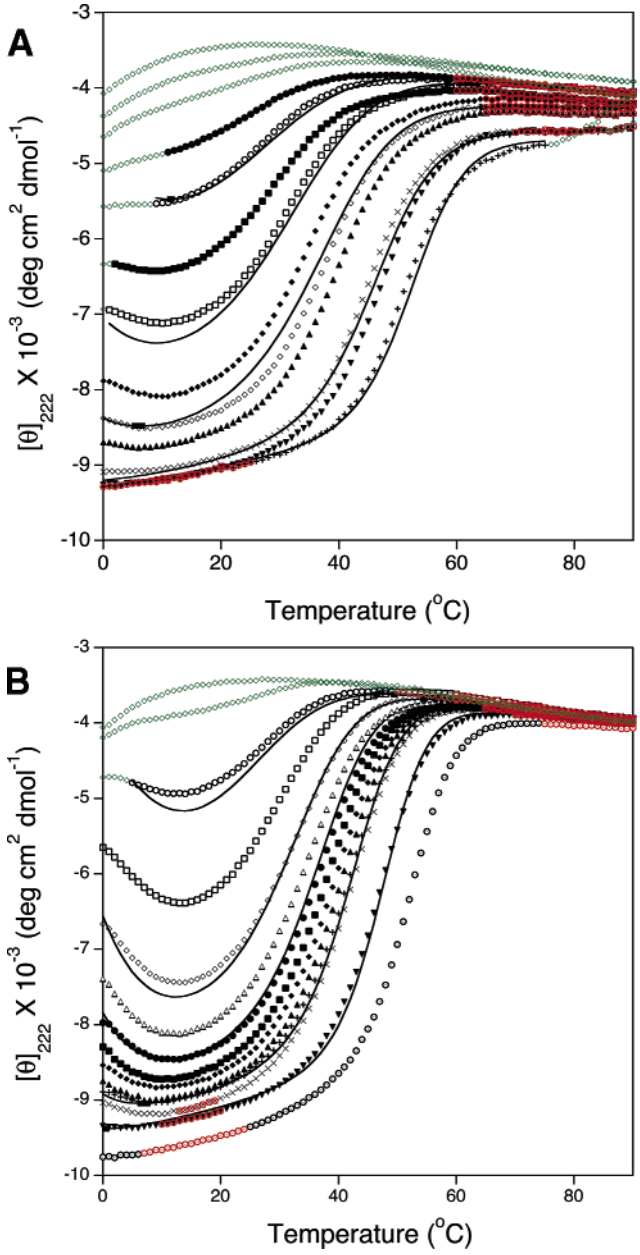

FIGURE 1: Far-UV CD thermal denaturations of P protein (10 μM) at various amounts of (A) TMAO or (B) sulfate. The buffer for both thermal denaturation surfaces is 10 mM sodium cacodylate, pH 7. The TMAO concentrations in panel A are 0.32 M (●), 0.44 M (○), 0.56 M (■), 0.66 M (□), 0.72 M (◆), 0.83 M (◇), 0.91 M (▲), 1.15 M (×), 1.24 M (▼), and 1.44 M (+). The Na_2SO_4 concentrations in panel B are 0.1 mM (○), 0.2 mM (□), 0.3 mM (◇), 0.4 mM (△), 0.5 mM (●), 0.6 mM (■), 0.7 mM (◆), 0.8 mM (▲), 0.9 mM (+), 1.0 mM (×), 2.0 mM (▼), and 5.0 mM (⊙). The thermal denaturation data that were used to define the native and denatured base surfaces are highlighted in red, while the data that were not used in the surface analysis are in green. The solid lines are simulated from the thermodynamic parameters obtained from the global fits of the $\Delta G_{exp}(T,[TMAO])$ and $\Delta G_{exp}(T,[SO_4])$ surfaces (shown in Figure 2) to eqs 18 and 21 respectively; see text for details.

chosen to represent the base surfaces are highlighted in Figure 1 and were identified as linear in either the pre-transition and post-transition region of a particular thermal denaturation. The equations that were used to globally fit of the folded, $B_N(T,[per])$, and unfolded, $B_D(T,[per])$, base surface data are

$$B_N(T,[per]) = y_N(0\ °C, 0) + b^T{}_N T + b^P{}_N[per] \quad (5)$$

$$B_D(T,[per]) = y_D(80\ °C, 0) + b^T{}_D(T)T + b^P{}_D[per] + b^{T,P}T[per] \quad (6)$$

where $y_N(0\ °C, 0)$ is the intercept of the folded base surface and $b^T{}_N$ and $b^P{}_N$ are the temperature (T) and perturbant ([per]) slopes of the folded base surface, respectively. Likewise, $y_D(80\ °C, 0)$ and $b^T{}_D$ and $b^P{}_D$ are the intercept and slopes of unfolded base surface with an additional cross term, $b^{T,P}$, which is required to adequately fit the unfolded base surface data (see Figure 1). However, the unfolded base surface of the TMAO thermal denaturation curves were not well-fit to eq 6 because an irreproducible systematic error in the blank cell signal precluded a global fit. Therefore, for these data, the post-transition region of each thermal denaturation in the osmolyte-surface was fit to a line to define the temperature dependence of the unfolded state (see Table 1 of Supporting Information for all best-fit base surface parameters).

In the second step of analysis, the thermal denaturation surfaces are converted to protein stability curves (ΔG_{exp} vs T plots, (*33*)) using eqs 2−6. The resulting protein stability curves for P protein in the presence of increasing TMAO and sulfate concentrations are shown in Figure 2 panels A and B, respectively. The useful transition region yields standard free-energy data that range from approximately +2 to −2 kcal/mol. Outside of this range, the free-energy uncertainty is very large because the CD signal differs only slightly from the native or denatured state signals.

There are several initial observations that can be made from the data in Figure 2. (i) The stabilizing effect of both solvent additives on P protein is clearly evident in the shift of the stability curves from $\Delta G_{exp} < 0$ at low solute concentrations and low temperatures to $\Delta G_{exp} > 0$ at higher solute concentrations. (ii) The parabolic shape of the stability curves at intermediate concentrations of osmolyte (0.4356−0.9149 M) or ligand (0.1−0.9 mM) is easily recognized thanks to the presence of both high and low temperature unfolding. Therefore, it is possible to accurately estimate the critical thermodynamic parameters ΔC_p, T_S, and ΔH_S (or ΔG_S), which are the change in heat capacity of unfolding, the temperature of maximum stability, and the enthalpy (or Gibbs free energy) at T_S. Each of these three parameters has a unique effect on different features of the protein stability curve, allowing them to be determined independently. (iii) Qualitative inspection of the two free-energy surfaces shown in Figure 2 reveals a systematic difference in curvature, suggesting that the global ΔC_p of unfolding for the ligand-folded protein is higher than that for the osmolyte-folded protein because ΔC_p is the characteristic parameter that determines the curvature of the stability curve parabola (i.e., $\delta^2\Delta G/\delta T^2 = -\Delta C_p/T$).

Conformational Stability of Osmolyte-Folded P Protein Using the Linear Free Energy of Interaction Model between TMAO and P Protein. The Gibbs−Helmholtz equation describing the standard free-energy unfolding reaction at any given temperature, $\Delta G(T)$, is

$$\Delta G(T) = \Delta H(T) - T\Delta S(T) \quad (7)$$

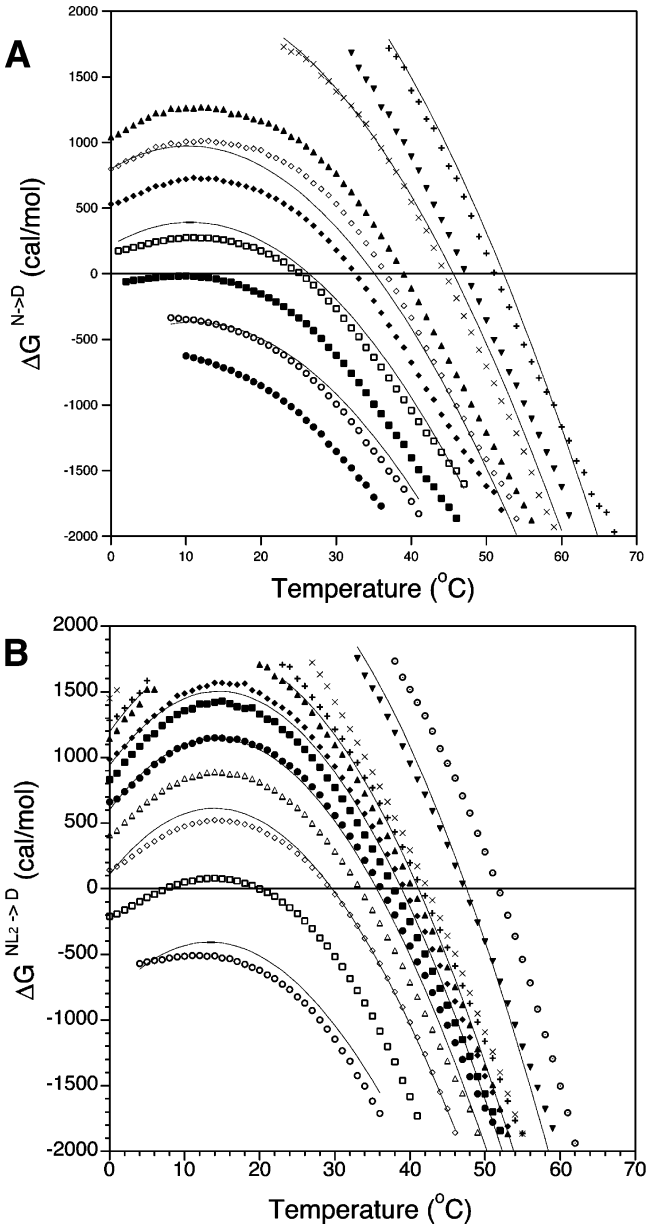

FIGURE 2: The free energy of unfolding (ΔG_{exp}) as a function of temperature at various concentrations of (A) TMAO or (B) sulfate. The data points correspond to those in Figure 1 using the transformation of eqs 2−6. The symbols are the same as in Figure 1: the TMAO concentrations in panel A are 0.32 M (●), 0.44 M (○), 0.56 M (■), 0.66 M (□), 0.72 M (◆), 0.83 M (◇), 0.91 M (▲), 1.15 M (×), 1.24 M (▼), and 1.44 M (+) and the Na_2SO_4 concentrations in panel B are 0.1 mM (○), 0.2 mM (□), 0.3 mM (◇), 0.4 mM (△), 0.5 mM (●), 0.6 mM (■), 0.7 mM (◆), 0.8 mM (▲), 0.9 mM (+), 1.0 mM (×), 2.0 mM (▼), and 5.0 mM (⊙). (A) The lines through the data represent the global fit of the entire TMAO protein stability surface using the unfolding thermodynamic parameters in Table 1. The best fit protein stability curves containing 0.44, 0.66, 0.83, 1.15, and 1.44 M TMAO are shown. (B) The lines through the data represent the global fit of the entire sulfate protein stability surface using the unfolding thermodynamic parameters extrapolated to 0 M TMAO (ΔH_S, T_S, ΔC_p) in Table 1 and the thermodynamic parameters for ligand dissociation (ΔH_{dis}, ΔS_{dis}, and $\Delta C_{p,dis}$) in Table 2 into eq 21. The best-fit protein stability curves containing 0.1, 0.3, 0.5, 0.7, 0.9, and 2 mM sulfate are shown.

where

$$\Delta H(T) = \Delta H(T_o) + \Delta C_p(T - T_o) \quad (8)$$

$$\Delta S(T) = \Delta S(T_o) + (\Delta C_p \ln(T/T_o)) \quad (9)$$

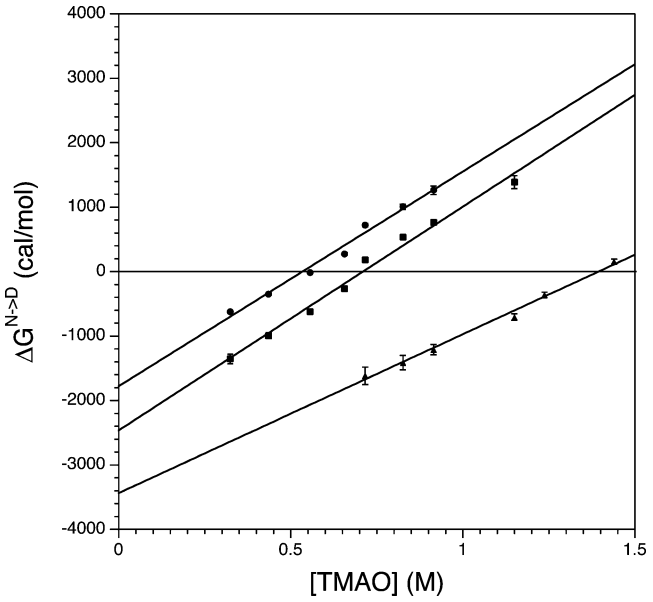

FIGURE 3: Osmolyte dependence of the free energy of unfolding, $\Delta G_{exp}(T)$, at 10 (●), 30 (■), and 50 °C (▲).The lines correspond to the linear least-squares fit to the data where the resulting best-fit slopes are 3.3 ± 0.2, 3.5 ± 0.2, and 2.5 ± 0.1 kcal mol^{-1} M^{-1} for 10, 30, and 50 °C, respectively.

Substituting eqs 8 and 9 into eq 7:

$$\Delta G(T) = \Delta H(T_o) - T\Delta S(T_o) + \Delta C_p(T - T_o - (T \ln(T/T_o))) \quad (10)$$

where $\Delta H(T)$ and $\Delta S(T)$ are the enthalpy and entropy of the system at a particular temperature T, and $\Delta H(T_o)$ and $\Delta S(T_o)$ represent the contributions to those thermodynamic parameters at the reference temperature T_o. In the following analysis, the temperature of maximum stability, T_S (where $\Delta S(T_S) = 0$), is used as the reference temperature so eq 10 reduces to

$$\Delta G'(T) = \Delta H_S' + \Delta C_p'(T - T_S' - (T \ln(T/T_S'))) \quad (11)$$

where ΔH_S is the enthalpy at T_S and corresponds to the maximum free energy (i.e., $\Delta H_S = \Delta G_S$). We assume that the Gibbs−Helmholtz equation holds under all buffer conditions, so the primes in eq 11 refer to a particular osmolyte or sulfate concentration.

The osmolyte dependence of ΔG_{exp} at several temperatures is shown in Figure 3. The standard free energy of protein unfolding appears to change linearly over the intermediate TMAO concentration range. Thus, the effect of osmolyte on the denaturation free energy of P protein is modeled using the linear free-energy relationship:

$$\Delta G([\text{TMAO}]) (= \Delta G') = \Delta G(0) - m_{os}[\text{TMAO}] \quad (12)$$

The standard free energy of the protein unfolding in the absence of osmolyte (0 M TMAO) is $\Delta G(0)$, and m_{os} is the unfolding free-energy dependence on molar concentrations of osmolyte. Note that the m_{os} value for the osmolyte is analogous to the m-values (m_{den}) used to describe the denaturant dependence of protein stability but has the opposite sign. Interestingly, the absolute value of m_{os} is approximately equal to the expected guanidinium chloride m-value (*29*) for a protein of P protein's size (118 amino

acids), which in turn is twice the magnitude for the expected urea *m*-value. This latter finding is important because the observed urea/TMAO concentration ratio for the cells that accumulate both small molecule osmolytes is about 2:1 (*34*). As shown by the best-fit lines in Figure 3, the commonly used linear extrapolation method (LEM) (*35*, *36*) can be employed to estimate the stability of the protein in the absence of osmolyte at various temperatures.

Figure 3 also shows that the best-fit values of m_{os} (slopes of the lines) are temperature-dependent (see Figure 1 of Supporting Information for a plot of m_{os} vs T based on globally fitted parameters). This observation indicates that osmolyte affects the thermodynamic parameters of P protein unfolding. One simple model that describes the influence of small molecule solutes on the thermodynamic parameters of unfolding is the linear free energy of interaction model originally proposed by Schellman and co-workers. This model predicts a linear dependence of enthalpy, entropy, and heat capacity on the perturbant concentration (*37*):

$$\Delta H' = \Delta H(0) - h[\mathrm{TMAO}] \quad (13)$$

$$\Delta S' = \Delta S(0) - s[\mathrm{TMAO}] \quad (14)$$

$$\Delta C_p' = \Delta C_p(0) - c[\mathrm{TMAO}] \quad (15)$$

The parameters *h*, *s*, and *c* are the slopes of the linear relationships between enthalpy, entropy, and heat capacity of unfolding and [TMAO]. These parameters can also be used to describe the temperature dependence of the free energy of the osmolyte−protein interaction, m_{os},

$$m_{os}(T) = h - Ts + c(T - T_o - (T \ln(T/T_o))) \quad (16)$$

The linear free-energy relationship between protein stability and TMAO concentration allows a global fit of the entire TMAO/temperature/protein stability surface data (Figure 2A) to ultimately determine the parameters that describe the osmolyte and temperature dependence of P protein stability in the absence of bound ligand. The generalized equation representing the free energy of the protein at any point within the temperature−osmolyte surface is obtained through the combination of eqs 10, 12, and 16:

$$\Delta G(T,[\mathrm{TMAO}]) = \Delta H(T_o) - T\Delta S(T_o) + \Delta C_p(T - T_o - (T \ln(T/T_o))) - m_{os}(T)[\mathrm{TMAO}] \quad (17)$$

Eq 17 has a total of eight thermodynamic parameters. To minimize the number of floating parameters, the point on the surface where the standard free energy, enthalpy, and entropy of denaturation are zero can be chosen for the reference temperature and osmolyte concentration, referred to hereafter as T_{HS} and C_{HS}. In general, this point is near the midpoint of both the thermal and osmolyte transitions, where ΔG can be most accurately estimated. When this reference point is used, the final global fitting equation simplifies to

$$\Delta G(T,[\mathrm{TMAO}]) = (h - Ts)[\mathrm{TMAO}]^* + (\Delta C_p + c[\mathrm{TMAO}]^*)\left\{T - T_{HS} - \left(T \ln\left(\frac{T}{T_{HS}}\right)\right)\right\} \quad (18)$$

where $[\mathrm{TMAO}]^* = [\mathrm{TMAO}] - C_{HS}$. The entire TMAO free-energy surface (Figure 2A, 418 points) was globally fitted using eq 18 to determine the reference point (T_{HS} and C_{HS}); *h*, *s*, and *c*; and ΔC_p. The temperature of maximum stability in the absence of osmolyte (T_S) can be calculated from these parameters as follows:

$$T_S = T_{HS} e^{(-s/[(c-\Delta C_p)/C_{HS}])} \quad (19)$$

Table 1: Thermodynamic Parameters of Unliganded P Protein Unfolding

parameter	fit value[a]	parameter (0 M TMAO)	extrapolated value[b]
ΔC_p	890 ± 23 cal mol^{-1} K^{-1}	ΔC_p	826 ± 32 cal mol^{-1} K^{-1}
T_{HS}	283.9 ± 0.4 K	T_S	284.9 ± 0.4 K
C_{HS}	0.543 ± 0.003 M	ΔH_S	-1864 ± 950 cal mol^{-1}
h	-4.9 ± 1.1 kcal mol^{-1} M^{-1}		
s	-5.3 ± 3.7 cal mol^{-1} K^{-1} M^{-1}		
c	-117 ± 43 cal mol^{-1} K^{-1} M^{-1}		

[a] The nonlinear global fit analysis of the data of the osmolyte/temperature/free energy surface in Figure 2A. There are a total of 418 points within the surface. The best fit parameters as well as the resulting standard errors from the nonlinear least-squares analysis are given. [b] Extrapolation to 0 M TMAO was carried out using the following relationships: (i) ΔC_p (0 M TMAO) = $\Delta C_p - c(0 - C_{HS})$; (ii) eq 19; and (iii) $\Delta H_S = \Delta G(T_S, 0\ \mathrm{M\ TMAO})$. Errors were propagated according to Bevington (*83*).

Table 1 displays the results of the global fitting analysis. Consistent with our previous observations (*23*), these thermodynamic parameters describe an unfavorable folding reaction in the absence of osmolyte or ligand. The latter state also represents a high-energy state along the coupled protein folding, ligand binding pathway. The standard free energy of unfolding is -1.9 ± 1.0 kcal/mol at 11.8 °C (T_S at 0 M TMAO), -2.1 ± 1.1 kcal/mol at 25 °C, -2.8 ± 1.1 kcal/mol at 37 °C, and -5.1 ± 1.1 kcal/mol at 60 °C. It should be noted that the uncertainties in $\Delta G(T)$ are quite large because proper error propagation (*83*) results in amplification of the uncertainties in ΔG when extrapolating from C_{HS} to 0 M TMAO. In contrast, the heat capacity change for this transition, which is 826 ± 32 cal mol^{-1} K^{-1}, is quite accurately determined because it is not strongly TMAO-dependent.

Conformational Stability of Ligand-Folded P Protein and Evidence for a Significant Contribution of Sulfate Binding to the Global ΔC_p. Sulfate-induced folding of P protein is a tightly coupled process involving the linked equilibria of protein folding and specific anion ligand binding. Given that anion-induced folding is a two-state process (*23*), the only populations that are observed in the transition region of a given thermal denaturation are the unliganded/unfolded and the liganded/folded states. Thus, it is not possible to uniquely assign the thermodynamics of protein folding and of ligand binding from the sulfate free-energy denaturation surface (Figure 2B) alone. In the following analysis, the parameters derived from the osmolyte-induced protein stability curves (Table 1) are used to determine the folding thermodynamics (ΔH_S, T_S, and ΔC_p) in the absence of ligand. Since the thermodynamics of P protein folding in the absence of either TMAO or sulfate can be assumed to be the same, the parameters defining the folding process under these conditions are held fixed, while those that describe the thermodynamics of binding (see

below) are allowed to float. This strategy has been used by us previously to extract the intrinsic binding constant of sulfate and other related anions to P protein at 37 °C (*23*) and is now extended to determine the binding constant at any temperature within the ligand free-energy surface shown in Figure 2B.

The apparent overall equilibrium constant describing the linked protein unfolding and ligand dissociation process is (*23*)

$$K_{app}([lig]) = K_U/(1 + K_d^{-1}[lig])^n \quad (20)$$

where K_U is the unfolding equilibrium constant in the absence of ligand, [lig] is the concentration of free ligand (SO_4), and K_d is the intrinsic dissociation constant for the n anion binding sites assuming the ligand binding sites are independent and have the same affinity. The corresponding apparent free energy of the coupled protein unfolding, ligand dissociation process is

$$\Delta G_{app}(T,[lig]) = -RT \ln(K_{app}(T,[lig])) = \Delta G(T) + nRT \ln(1 + K_d^{-1}[lig]) \quad (21)$$

where $\Delta G(T)$ is the unfolding free energy of the protein in the absence of sulfate. The second term in eq 21 describes the energetic effect of ligand dissociation on the global stability of the system. This term differs from the free energy of dissociation in simple binding reactions, which has the same form but lacks the addition of 1 to K_d^{-1}[lig]. The difference between the coupled and uncoupled binding reactions is that at [lig] $\ll K_d$ the binding contribution to the free energy of the folding/binding reaction is zero, whereas the free energy of a simple association reaction becomes strongly positive. In all samples containing sulfate, the ligand concentration is at least 10-fold larger than the experimental protein concentration; therefore, the total and free sulfate concentrations were assumed to be the same in the analysis. The conformational stability of P protein in the absence of sulfate has the form of eq 11, and the parameters (ΔH_S, T_S, and ΔC_p) defining unliganded P protein are given in Table 1. The temperature dependence of the sulfate dissociation constant can be ascertained through its relationship to the dissociation free energy, ΔG_{dis}.

$$K_d(T) = (\exp\{-\Delta G_{dis}(T)/RT\})/1000 \quad (22)$$

$$\Delta G_{dis}(T) = \Delta H_{dis}(T_o) - T\Delta S_{dis}(T_o) + \Delta C_{p,dis}(T - T_o - (T \ln(T/T_o))) \quad (23)$$

where ΔH_{dis}, ΔS_{dis}, and $\Delta C_{p,dis}$ are the enthalpy, entropy, and heat capacity changes associated with dissociation at the reference temperature T_o. The dissociation constant in eq 22 is defined in units of millimoles of ligand, and a favorable free energy of dissociation ($\Delta G_{dis} < 0$) contributes a negative free energy to the coupled unfolding/dissociation process, which is consistent with the formalism established in the previous section.

The equation used to globally fit the sulfate free-energy surface is obtained by substituting eqs 22 and 23 into eq 21. The fitted parameters are ΔH_{dis}, ΔS_{dis}, and $\Delta C_{p,dis}$. The number of ligand binding sites, n, was also a parameter allowed to float in a preliminary nonlinear least-squares fit of the ligand/temperature/protein stability surface data. The best-fit n was determined to be 1.81 ± 0.02 sulfate molecules with insignificant cross-correlation to the parameters describing the thermodynamics of ligand dissociation (data not shown). This result is in agreement with our previous finding that the number of pyrophosphate binding sites that induce folding is two under stoichiometric binding conditions (*23*). The current results indicate that this conclusion extends to sulfate, which does not bind stoichiometrically to P protein under our conditions. Table 2 shows the results of the global fitting analysis of the sulfate free-energy surface (Figure 2B), where the number of ligand binding sites was fixed to two. These parameters are the same within error to those when n is allowed to float (data not shown). The best-fit parameters in Tables 1 and 2 were used to generate the stability curves shown with the experimental data in Figure 2B. The best-fit values indicate a modest temperature dependence of the sulfate dissociation constant in the physiological temperature range (45 ± 23 μM at 25 °C, 68 ± 34 μM at 37 °C, 288 ± 138 μM at 60 °C), but it rises sharply at temperatures above 60 °C (see Supporting Information, Figure 2). An exothermic enthalpy of dissociation is found over most of the observed temperature region in the surface ($\Delta H_{dis} > 0$ when $T > 13$ °C; i.e., $T_{H,dis} \sim 13$ °C), which may be due to favorable ionic interactions between the bound sulfate ions and the positively charged P protein surface.

Table 2: Thermodynamic Parameters of Sulfate Dissociation from Liganded P Protein

parameter[a]	fit value
ΔH_{dis}	-444 ± 150 cal mol^{-1} M^{-1}
ΔS_{dis}	-21.8 ± 0.5 cal mol^{-1} K^{-1} M^{-1}
$\Delta C_{p,dis}$	363 ± 9 cal mol^{-1} K^{-1} M^{-1}
K_d (25 °C)	44.6 ± 2.3 μM
K_d (37 °C)	68.4 ± 3.5 μM
K_d (60 °C)	288 ± 17 μM

[a] The parameters defining the temperature dependence of K_d, ΔH_{dis}, ΔS_{dis}, and $\Delta C_{p,dis}$ were determined through nonlinear fit of the sulfate/temperature/free energy data (shown in Figure 2B, 494 points) to eq 21. The parameters defining the protein unfolding thermodynamics (ΔC_p, T_S, ΔH_S) were fixed to the values given in Table 1. The best-fit values and the resulting standard error from the nonlinear least-squares global fitting analysis are shown. The intrinsic sulfate dissociation constants were calculated at the displayed temperatures using eq 22 with the appropriate propagated errors.

A large value of $\Delta C_{p,dis}$ is required to fit the increased curvature found in the sulfate-induced stability curves relative to the TMAO-induced curves (Figure 2). In accordance with global fit analysis (Table 2), the dissociation of a sulfate results in a heat capacity change of 363 cal mol^{-1} K^{-1} M^{-1} per site. However, it is not obvious how this relatively large value of $\Delta C_{p,dis}$ contributes to the enhanced curvature for the sulfate stability curves from the global fitting equation (eq 21). To understand the contribution of the ligand binding parameters (ΔH_{dis}, ΔS_{dis}, $\Delta C_{p,dis}$) on the apparent global ΔC_p for the coupled unfolding−ligand dissociation reaction, $\Delta C_{p,app}(T,[lig])$, the experimental stability curves generated at various sulfate concentrations in Figure 2B were fit to eq 11. In this case, the primes reflect the thermodynamic values evaluated at a particular ligand concentration. The resulting fit $\Delta C_{p,app}$ values at each sulfate concentration are shown in

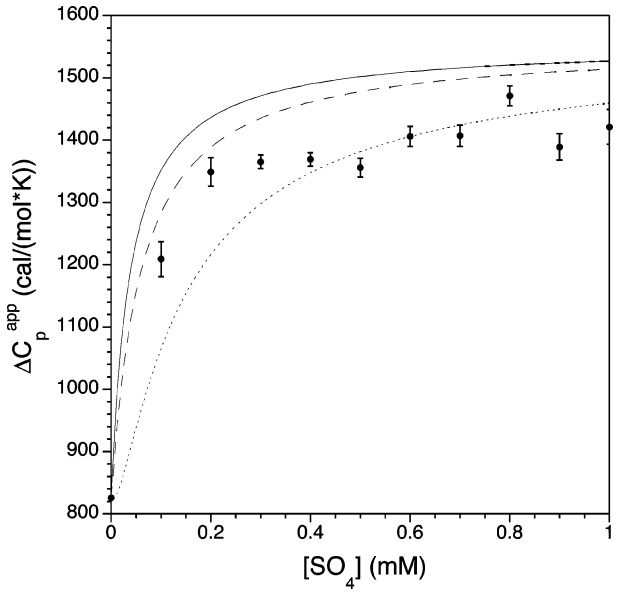

FIGURE 4: The global heat capacity difference for the coupled protein unfolding and ligand dissociation reaction, $\Delta C_{p,app}$, has an apparent ligand dependence as well as a temperature dependence. The $\Delta C_{p,app}$ is defined as $-T\delta^2\Delta G/\delta T^2$, where $\Delta G = \Delta G(T,[SO_4])$, the global fitting equation for the ligand-bound protein free energy surface shown in eq 21. The lines represent the predicted dependence of ΔC_p^{app} at 11.8 °C (solid line, T_S of P protein in the absence of TMAO), 25 °C, (dashed line), and 37 °C (dotted line) using the best-fit parameters for unfolding (Table 1) and ligand binding (Table 2). The data points represent the resulting $\Delta C_p'$ values when the individual protein stability curves in Figure 2B are fit to the Gibbs−Helmholtz equation (eq 11).

Figure 4. The equation that describes the sulfate dependence of $\Delta C_{p,app}$ is

$$\Delta C_{p,app}(T,[lig]) = -T(\delta^2\Delta G_{app}(T,[lig])/\delta T^2) \quad (24)$$

substituting ΔG_{app} as defined in eq 21 and evaluating the derivative

$$\Delta C_{p,app}(T,[lig]) = \Delta C_p + \{2K_d^{-1}[lig]/(1 + K_d^{-1}[lig])\}[\Delta C_{p,dis} + (\Delta H_{dis} + \Delta C_{p,dis}(T - T_o))^2/((1 + K_d^{-1}[lig])RT^2)] \quad (25)$$

This equation is plotted for $T = 11.8$, 25, and 37 °C in Figure 4. Intriguingly, the apparent ΔC_p for the coupled unfolding/ligand dissociation reaction is strongly ligand concentration- and temperature-dependent. In the absence of ligand, $\Delta C_{p,app}$ starts at 826 cal mol^{-1} K^{-1} and rises to a standard state (1 M) $\Delta C_{p,app}$ of 1554 cal mol^{-1} K^{-1}; the standard state value is roughly equivalent to $\Delta C_p + 2\Delta C_{p,dis}$. Because the last term in eq 25 is small compared to $\Delta C_{p,dis}$, $\Delta C_{p,app}$ displays the shape of a binding curve for two independent binding sites. Thus, $\Delta C_{p,app}$ is an observable parameter that can be used to monitor the fraction of folded P protein bound to the sulfate ligand. The apparent temperature dependence of $\Delta C_{p,app}$ is primarily due to the fact that the intrinsic binding constant is temperature-dependent as shown in Table 2. Overall, $\Delta C_{p,app}$ increases approximately 88% in the progression from the unliganded N conformation to the folded conformation in the presence of standard state concentrations of ligand (NL_2, 1 M SO_4). For this reason, there is a significant difference between the extrapolated values of ΔC_p for the osmolyte-folded and the ligand-folded conformational states of P protein.

DISCUSSION

CD Thermal Denaturation Surfaces Give Folding and Ligand Binding Thermodynamics of an IUP. To understand the molecular interactions responsible for the structure of a protein, an accurate determination of the unfolding thermodynamics is required in addition to a high-resolution structure model. Indeed, given the relative success of the field of structural energetics to predict protein binding free energies (reviewed in ref *38*), cooperative folding units (*39*), and amide hydrogen exchange protection factors (*40*, *41*), it is possible to relate structural changes to thermodynamics. One of the most reliable structure/thermodynamic correlations is between ΔC_p and ΔASA. Thus, the determination of ΔC_p can provide structural clues to the alterations upon thermal unfolding. Unfortunately, elevated temperatures lead to little or no change in structure for the IUP class of proteins, as assayed by biophysical techniques (*2*, *42*).

To get an estimate of the folding thermodynamics of an IUP, the protein must be stabilized in some manner so that a cooperative thermal unfolding transition can be observed. Two different solvent additives that act upon the protein in differing ways can achieve such stabilization for P protein (Figure 1). The resulting stability curves (Figure 2) arise from a temperature-dependent conformational free energy of a protein (*33*), which is a function of the conformational enthalpy, entropy, and heat capacity (eq 10). The temperature dependence of these thermodynamic properties can be calculated from three parameters: T_S, ΔH_S, and ΔC_p, each of which controls the shape of the stability curve in a unique manner (see Figure 3 in ref *43*). In this study, we determined the stability curves for two folded forms of P protein over a wide range of stabilities attained through addition of either TMAO (osmolyte) or Na_2SO_4 (ligand). This method results in a CD thermal denaturation surface where both temperature and buffer additive concentration are the independent axes, while the CD signal is the dependent axis. To the best of our knowledge, this is the first time that an intrinsically unstructured protein has been analyzed via CD thermal denaturation surfaces with an osmolyte to elicit stability curves.

Accurate determination of the parameters that define the stability curve, particularly ΔC_p, requires the observation of both heat and cold denaturation within the experimentally accessible transition region (*37*). The stability curves shown in Figure 2 clearly display both heat and cold denaturation within this free-energy window in the presence of either the renaturant TMAO or the ligand sulfate. There are several assumptions implicit in this analysis. First, the two unfolded states, the high-temperature denatured state at all perturbant concentrations and the cold denatured state observed at intermediate osmolyte/ligand are treated as thermodynamically the same state. This assumption is based on previous findings that the thermodynamic properties of native proteins are consistent regardless of denaturing perturbant (reviewed in ref *44*). The second assumption is that the thermal unfolding transition can be described as a two-state process throughout the perturbant-temperature free-energy surface

and involves only two thermodynamic ensembles, referred to here as the native and denatured states.

Despite these assumptions, there are several advantages of using CD denaturation surfaces to determine thermodynamic parameters: (i) the low required protein concentrations minimize aggregation, (ii) the relatively high degree of reversibility for this technique, and (iii) constant pH avoids any pH-dependent effects. The principal disadvantage of this technique is that the enthalpy and heat capacity are derived from the first and second derivatives of the protein stability curve and are not directly measured observable. Recently, DSC has been used to estimate the absolute heat capacity of unfolded protein fragments, which, when combined with a calculation of the absolute heat capacity of the fully solvated unfolded state, yields the ΔC_p of natively disordered fragments (*45*, *46*). However, this method requires that the protein is monomeric at concentrations $>50\ \mu$M; this is not the case for unliganded, unfolded P protein as assayed by PFG-NMR experiments (C.H.H. and T.G.O., unpublished observations). Therefore, CD thermal denaturation studies serve as the most appropriate technique to study the thermal unfolding transition of P protein when stabilized by TMAO or ligand.

Unliganded, Folded P Protein (N) Has a Less Favorable Enthalpy and a Lower ΔC_p of Unfolding Than Stable Proteins Its Size. In low ionic strength buffer, P protein's lowest energy conformation is best characterized as predominantly unfolded. The addition of anionic ligands causes a major structural rearrangement coincident with a transition to a state whose CD spectrum is consistent with the mixed α/β conformation observed in crystallographic and NMR studies (*47*−*49*). Experimental evidence suggests that this ligand-induced transition is two-state so that the only conformational ensembles that are observed are the unliganded, denatured (D) and the liganded, native (NL_2) states. Therefore, the unliganded, native (N) ensemble is a poorly populated high-energy state (*50*) along the coupled, folding binding pathway. We previously determined the free energy of N relative to D by extrapolating TMAO renaturation curves to 0 M osmolyte (*23*). Here, we further dissect the energetic basis for the disfavored N conformation into enthalpic and entropic components. In a broader context, high-energy conformations can represent active/activated conformations of enzymes or protein receptors that are poorly populated in the absence of their substrate/ligand. In particular, so-called "induced-fit" binding is an example of a process where such high-energy conformations play a key role.

P protein has a stability of −2.1 kcal/mol, which corresponds to a mole fraction of 2.8% for the unliganded N state at 25 °C in 10 mM sodium cacodylate buffer (pH 7). Figure 3 demonstrates that the observed free energy (ΔG_{exp}) is a linear function of [TMAO] with a slope defined as m_{os}. The empirical linear relationship between osmolyte concentration and protein stability has been observed (*51*) or assumed elsewhere (*52*−*54*) and has been rationalized theoretically (*55*). Alternative nonlinear models for the free-energy interaction between osmolyte/denaturant and protein have been described (*51*, *56*−*58*), but the linear free-energy model is the simplest model to fit the data. Another intriguing finding is that the magnitude of m_{os} is quite large, −3320 cal mol^{-1} M^{-1} at 25 °C. This value is of opposite sign and the same magnitude as the predicted *m*-value of guanidine chloride for a protein of P protein's size using the correlation of Myers et al. (*29*). Thus, this osmolyte is a very strong renaturant for P protein folding.

There are two limiting ways to energetically stabilize the unfolded form of an IUP (eq 7). An unusually low folding enthalpy (ΔH) coupled with a typical folding entropic energy ($T\Delta S$) can achieve this result. Alternatively, an uncharacteristically high $T\Delta S$ that overwhelms a representative folding ΔH will also yield the same phenomenon. Since the unfolding thermodynamics of P protein are monitored only in the presence of osmolyte, the affect of TMAO upon the apparent enthalpy, entropy, and heat capacity must be determined in order to reveal the thermodynamic basis of P protein's tendency to unfold in the absence of ligand. In our analysis, we use the linear free-energy interaction model (eqs 12−16) to calculate the thermodynamic parameters of P protein stability in the absence of osmolyte (Table 1). Thus, the enthalpic and entropic contributions to the unfolding free energy of the ligand-free N → D transition can be determined and are shown in Figure 5A. In the absence of osmolyte at 25 °C, the free energy of folding is 2.1 kcal/mol, which is the result of a favorable folding enthalpy of −9.1 kcal/mol that is too small to offset the large positive contribution (11.2 kcal/mol) arising from a folding-associated loss in entropy. Using the empirical correlations reported by Murphy and Robertson (Table 5 in ref *28*), we expect a 118-residue stable protein might have a folding free energy of about −5 kcal/mol due to a favorable enthalpy of ∼−25 kcal/mol that outweighs the unfavorable entropic contribution of ∼20 kcal/mol at 25 °C. Since this estimate is twice our measured value, the low stability of N must be due primarily to a low enthalpy of folding, which is much lower than that for stable proteins. One likely cause for low folding enthalpy is the presumed increase in charge density concomitant with the folding of a highly basic protein (pI ∼ 10.2, net charge of +17 at pH 7 (*59*)). Indeed, a common characteristic of IUPs is a high mean net charge and low mean net hydrophobicity (*60*).

Interestingly, the ΔC_p of TMAO-induced folding of P protein at C_{HS} is 890 cal mol^{-1} K^{-1}; a value significantly lower than the prediction based on the surface exposure of the native structure of P protein (see below). Significantly depressed ΔC_p values have been reported for proteins in the presence of molar concentrations of osmolytes (*61*, *62*) as well as stabilizing carboxylic salts (*63*). An intriguing explanation for the reduction of ΔC_p in the presence of these solvent additives arises from the observation that denatured proteins have been found to be more compact in the presence of molar quantities of osmolytes (*64*). Therefore, the compaction of the denatured state *due to the presence of osmolyte* may result in the lower ΔASA between the end states in the thermal unfolding transition of Figure 2A. Although this is an interesting explanation, the following observations do not support this hypothesis. The ΔC_p of 826 cal mol^{-1} K^{-1} is an extrapolation to 0 M TMAO as described by the linear free-energy relationship (eq 15); therefore, the effect of solute on either end state is removed. Additionally, if there is preferential compaction of the denatured state relative to the native state and this effect is concentration-dependent, then the prediction would be flatter free-energy curves as the concentration of TMAO increases. Experimentally, this phenomenon is not observed (Figure 2A), rather

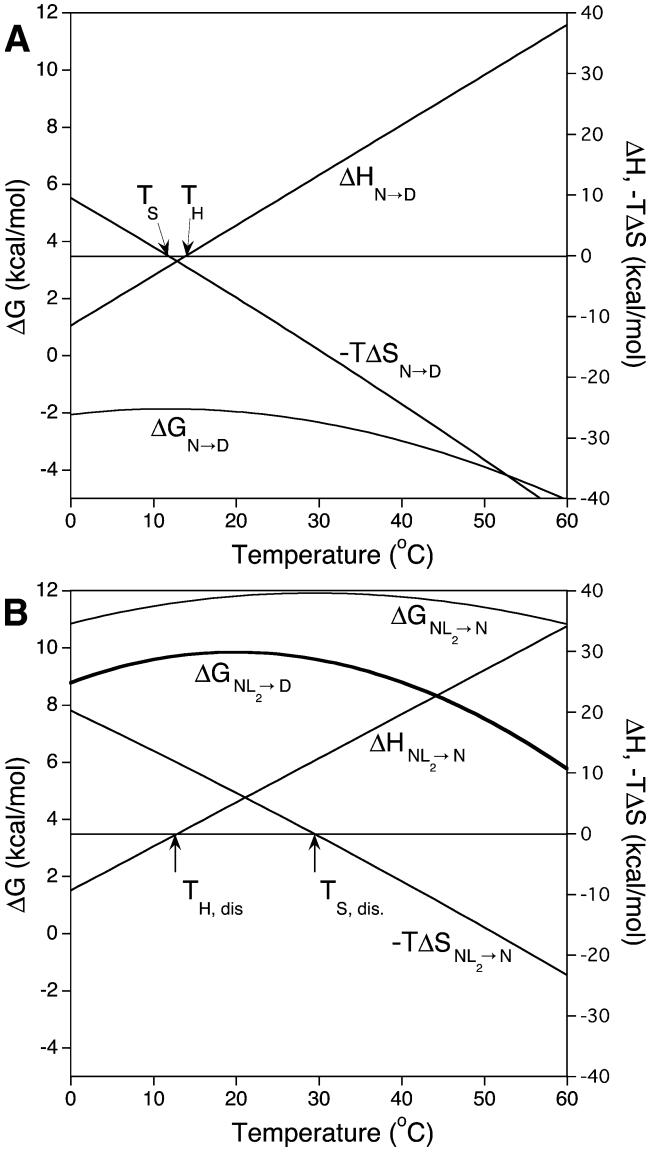

FIGURE 5: (A) Dissecting the free energy of unfolding of the N → D transition, $\Delta G_{N\rightarrow D}$, into its enlthalpic and entropic components. The conformational stability ($\Delta G_{N\rightarrow D}$) of P protein, and the contributions of enthalpy (ΔH) and entropy ($-T\Delta S$) are shown over the given temperature range (0−60 °C). T_S, the temperature of maximum stability, and T_H, the temperature where ΔH is zero, are 11.8 and 14.0 °C, respectively. (B) Breakdown of the free energy of sulfate dissociation, $\Delta G_{NL2\rightarrow N}$, into enthalpic and entropic components. The lines representing the temperature dependence of the dissociation free energy, enthalpy, and entropy at 1 M are analogous to those in panel A. $T_{H,dis}$ and $T_{S,dis}$ are calculated to be 13.0 and 29.3 °C, respectively. The bold solid line represents the apparent conformational stability of P protein in the presence of 1 M ligand.

the opposite is observed as the TMAO dependence of ΔC_p, *c*, is −117 cal mol^{-1} K^{-1} M^{-1} (Table 2).

An Enthalpic Ligand Binding Reaction Compensates for Low Enthalpy of High-Energy Intermediate Formation. Visual comparison of the stability curves for P protein in the presence of sulfate reveals a greater curvature than was observed in the presence of TMAO (Figure 2). This observation provides strong qualitative evidence that the ΔC_p of the unfolding and sulfate dissociation reaction is significantly larger than the ΔC_p of the unfolding reaction alone. Using the folding parameters in Table 1, we show in Table 2 the best-fit parameters describing the dissociation thermodynamics along with the intrinsic sulfate dissociation constant. Not surprisingly, the sulfate binding constant is several orders of magnitude weaker than that determined for P RNA, its in vivo binding partner (*15*, *65*).

The thermodynamic parameters that define the temperature dependence of intrinsic binding constants reveal the energetic contributions of the P protein−sulfate ion interaction. The large temperature dependence of both the enthalpy and the entropy (due to a large $\Delta C_{p,dis}$) leads to a change in driving force over the physiological temperature range. As depicted in Figure 5B, the free energy of association is entirely entropic at $T_{H,dis}$ (13 °C), while it is entirely enthalpic at $T_{S,dis}$ (29.3 °C), the temperature of maximum intrinsic affinity. Below this temperature range, association is driven by a favorable entropy change, whereas above 30 °C, association is driven by a favorable enthalpy change. In general, a favorable association enthalpy is observed over the physiological temperature range and constitutes the larger energetic contribution toward the stabilization of the high-energy N state of P protein when ligand binds. Thus, the unusually low enthalpy of the folding to the unliganded conformation of P protein is compensated by the enthalpy gained upon ligand binding. One likely contribution to this enthalpy gain is formation of salt bridges between the sulfate ions and the basic side chains of P protein, which would have their own favorable enthalpy while also neutralizing enthalpically unfavorable charge−charge repulsion. Other potential contributions to a favorable enthalpy include the hydration of charged or polar groups (*25*), or hydrogen bond formation (*66*) as a result of ligand binding. Furthermore, a favorable enthalpy is commonly observed in other charged macromolecular associations such as protein−DNA interactions; that is, $T_{H,bind} \sim 6-20$ °C (*67*, *68*).

The increase in the curvature of the stability curves caused by addition of sulfate suggests that there is a significant ΔC_p associated with ligand binding (Figure 2). For sulfate binding to P protein, the best-fit $\Delta C_{p,dis}$ is 363 cal mol^{-1} K^{-1} M^{-1} for the dissociation reaction for each ligand site. The extrapolated $\Delta C_{p,app}$ at 25 °C under standard state conditions (1 M sulfate) is 1554 cal mol^{-1} K^{-1}, which corresponds to approximately an 88% increase in the ΔC_p relative to the high-energy N state. Because the apparent heat capacity change for the coupled folding/binding reaction depends on the fraction of protein molecules with ligand bound, $\Delta C_{p,app}$ is ligand- and temperature-dependent as described by eq 25 (Figure 4). Another interesting finding is that the ΔC_p values in the saturated portions of the binding isotherms ([ligand] > 5 mM sulfate) are about $\Delta C_p + 2\Delta C_{p,dis}$, or 1554 cal mol^{-1} K^{-1}, which is well-predicted by the structure-based relationship of eq 1 (see below).

The Large Difference in Heat Capacity between N and NL$_2$ Is Not Exclusively Due to Burial of Surface Area. The correlation between ΔC_p and ΔASA remains one of the most useful relationships in the field of structural energetics (*25*, *26*, *28*). Assuming an extended chain solvent accessibility for the unfolded state (*69*), the unfolding ΔC_p of any protein whose structure is known can be predicted using eq 1. Christensen and co-workers have solved the crystal structure of the *B. subtilis* P protein (*47*) (pdb file 1A6F) used in this study. COREX (*40*) was used to calculate the ASA of the folded and unfolded states giving ΔASA values of 6854 Å^2

and 4520 Å^2 for the apolar and polar surface, respectively. Thus, the ΔC_p of unfolding P protein is predicted to be between 1.5 and 1.9 kcal mol^{-1} K^{-1} depending upon which heat capacity coefficient constants are used (*26*).

A primary goal of this study was to discern from the ΔC_p values of P protein refolded in either TMAO or sulfate whether there are structural differences in the two folded forms. An interesting conundrum arises when one compares the extrapolated ΔC_p values for P protein refolded in 2 M TMAO and 20 mM sulfate using the parameters from Table 1 and Table 2, respectively. The apparent ΔC_p for P protein refolded in 2 M osmolyte is 1060 cal mol^{-1} K^{-1}, while the value for P protein refolded in ligand is ~1552 cal mol^{-1} K^{-1}; this yields a ΔC_p ratio of ~0.68. In accordance with the correlation between ΔC_p and ΔASA, osmolyte-folded P protein would be predicted to bury two-thirds of the total protein surface area that is buried in the sulfate-refolded protein. However, it is not likely that 32% of the protein surface (or 38 residues) is solvated in the osmolyte-folded form while not in the ligand-folded form given the spectral similarities of the far- and near-UV CD and HSQC spectra between the two conformations (*23*). Additional evidence for the similarity of accessible surface area of the two folded forms of P protein comes from its sensitivity to osmolyte. The denaturant *m*-value is strongly correlated with the ΔASA of chemical denaturation (*29*). Furthermore, Bolen and co-workers have shown that TMAO can counteract destabilization of urea in an independent and additive manner where the protein stability is unaffected when the counteracting solvents are at an approximate 2:1 urea/TMAO molar ratio (*32*). This observation is consistent with the average TMAO/urea *m*-value ratio observed of −1.7 for Barnase and the Notch ankyrin domain (*70*). Urea denaturation of P protein refolded in 20 mM Na_2SO_4 gave an m_{den} value of 1990 ± 50 cal mol^{-1} M^{-1} at 25 °C (data not shown). Multiplying this value by −1.7 gives a predicted m_{os} value of −3400 cal mol^{-1} M^{-1} for the $NL_2 \leftrightarrow$ D transition. The observed m_{os} for the N ↔ D transition at 25 °C is −3300 cal mol^{-1} M^{-1} indicating that folding of unliganded N buries 97% of the area buried in NL_2. Taken together with the spectroscopic data, these observations suggest that unliganded N has structure and solvent accessibility very similar to that of NL_2. Therefore, other explanations must be pursued to account for this large ΔC_p discrepancy.

Despite the structural similarities of the unliganded and liganded native forms, the unfolding ΔC_p of N is 826 cal mol^{-1} K^{-1}, while that of NL_2 is 1554 cal mol^{-1} K^{-1}. One obvious difference between the two folded conformations is the presence of the bound sulfate anions. However, the amount of protein surface buried per sulfate is about 100 Å^2 (*71*), most of which buries polar side chain groups. This process is predicted to decrease rather than increase $\Delta C_{p,app}$.

Significant disparities between experimental ΔC_p and ΔC_p predicted from surface area estimates for ligand association reactions have been observed in many DNA−protein (*67*, *72*−*74*) and protein−ligand (*75*, *76*) interactions. In some cases, the inclusion of an "induced-fit" conformational change of the protein, which results in additional surface burial, is sufficient to account for the ΔC_p deficit (*77*, *78*) or at least come closer to the experimental ΔC_p (*75*). By analogy, we searched for a region on P protein that may add buried protein surface upon sulfate binding. One sulfate ion observed in the *B. subtilis* P protein crystal structure (*47*) is coordinated by three residues (H3, R9, and R68), two of which are in the N-terminal region. Interestingly, the analogous N-terminal region of *S. aureus* P protein is not well-constrained in the solution structure, which was solved in a buffer containing a weak affinity Cl^- ion (*48*). Thus, if it is assumed that the N-terminal region (liberally defined as A2−D15; *B. subtilis* numbering) is unfolded in the absence of sulfate, the osmolyte-folded protein would expose an additional ~1238 Å^2 of protein surface, 714 Å^2 apolar surface, and 524Å^2 polar surface relative to the liganded protein. The predicted increase in unfolding ΔC_p upon the release of sulfate is only 150−190 cal mol^{-1} K^{-1}. Therefore, the observed increase in ΔC_p of unfolding between osmolyte-folded and ligand-folded P protein (~500 cal mol^{-1} K^{-1}) cannot be entirely accounted for by this putative induced conformational change.

Other potential positive contributions to $\Delta C_{p,app}$ of the coupled protein unfolding-ligand dissociation reaction have been proposed. These include electrostatic contributions to the heat capacity, ΔC_p^{el}, (*79*) which could arise from protein−ion association at elevated sulfate concentrations or the dehydration of solvent ions (*72*), such as cacodylate, sulfate, or acetate that bind nonspecifically to the basic highly basic P protein upon unfolding. However, these contributions would be relatively insignificant (<100 cal mol^{-1} K^{-1}) compared to the large ΔC_p difference between osmolyte-folded and ligand-folded P protein.

The only other previously proposed mechanism for additional contribution to ΔC_p is a "tightening of the soft vibrational modes" (*30*) of the protein, ligand, or water molecules. Ladbury and co-workers have further adapted this idea to suggest that regions that restrict the motion of water molecules upon the burial of stereospecific polar interaction surfaces could have a significant effect on the measured heat capacity (*67*, *80*). The latter interpretation that the trapping of water can lead to significant heat capacity effects is also supported by recent lattice models (*81*). An analysis of *B. subtilis* crystal structure reveals that there are 10 assigned H_2O molecules, one of which was proposed to represent the second sulfate (H_2O 500). Unfortunately, there is no extensive buried water-mediated hydrogen-bonding network around the assigned and/or presumed sulfate anions. Furthermore, the water molecules appear to be well-distributed throughout the surface of the protein. However, the possibility of additional bound waters in ligand-folded P protein that are absent in the osmolyte-folded protein cannot be excluded.

Further investigation is required to ascertain whether the "stiffening" of vibrational modes in the protein, ligand, or water provides an adequate molecular representation of the difference in the ΔC_p value between the two folded states. Regardless of mechanism, we attribute a large portion of the difference in the ΔC_p of the two folded states to differences in the conformational heterogeneity of the two ensembles arising from differences in the soft vibrational modes (500−800 cm^{-1}) between N and NL_2. Specifically, a ΔC_p increment may arise if the presumed high-frequency conformational fluctuations in N are dampened/stiffened upon binding ligand; thus, NL_2 would be more tightly packed, or less liquidlike, than N. Recently, such evidence for the presence of conformational heterogeneity has been proposed for the native state ensemble of ubiquitin (*82*).

ACKNOWLEDGMENT

We thank Dr. Jeffrey K. Myers for critically reading the manuscript, various members of the Oas laboratory for helpful discussions and advice, and an anonymous reviewer for alerting us to an additional source of large "anomalous" heat capacity effects.

SUPPORTING INFORMATION AVAILABLE

Table S1 showing the best-fit base surface parameters and figures showing the plot of m_{os} versus T (Figure S1) and K_d versus T (Figure S2) based on globally fitted parameters. This material is available free of charge via the Internet at http://pubs.acs.org.

REFERENCES

1. Wright, P. E., and Dyson, H. J. (1999) Intrinsically unstructured proteins: re-assessing the protein structure−function paradigm, *J. Mol. Biol. 293*, 321−331.
2. Uversky, V. N. (2002) Natively unfolded proteins: a point where biology waits for physics, *Protein Sci. 11*, 739−756.
3. Tompa, P. (2002) Intrinsically unstructured proteins, *Trends Biochem. Sci. 27*, 527−533.
4. Dunker, A. K., Lawson, J. D., Brown, C. J., Williams, R. M., Romero, P., Oh, J. S., Oldfield, C. J., Campen, A. M., Ratliff, C. M., Hipps, K. W., Ausio, J., Nissen, M. S., Reeves, R., Kang, C., Kissinger, C. R., Bailey, R. W., Griswold, M. D., Chiu, W., Garner, E. C., and Obradovic, Z. (2001) Intrinsically disordered protein, *J. Mol. Graphics Modell. 19*, 26−59.
5. Dunker, A. K., Brown, C. J., Lawson, J. D., Iakoucheva, L. M., and Obradovic, Z. (2002) Intrinsic disorder and protein function, *Biochemistry 41*, 6573−6582.
6. Dyson, H. J., and Wright, P. E. (2002) Coupling of folding and binding for unstructured proteins, *Curr. Opin. Struct. Biol. 12*, 54−60.
7. Koshland, D. E. (1958) Application of a theory of enzyme specificity to protein synthesis, *Proc. Natl. Acad. Sci. U.S.A. 44*, 98−104.
8. Lydakis-Simantiris, N., Hutchison, R. S., Betts, S. D., Barry, B. A., and Yocum, C. F. (1999) Manganese stabilizing protein of photosystem II is a thermostable, natively unfolded polypeptide, *Biochemistry 38*, 404−414.
9. Shoemaker, B. A., Portman, J. J., and Wolynes, P. G. (2000) Speeding molecular recognition by using the folding funnel: the fly-casting mechanism, *Proc. Natl. Acad. Sci. U.S.A. 97*, 8868−8873.
10. Kriwacki, R. W., Hengst, L., Tennant, L., Reed, S. I., and Wright, P. E. (1996) Structural studies of p21Waf1/Cip1/Sdi1 in the free and Cdk2-bound state: conformational disorder mediates binding diversity, *Proc. Natl. Acad. Sci. U.S.A. 93*, 11504−11509.
11. Lei, M., Lu, W., Meng, W., Parrini, M. C., Eck, M. J., Mayer, B. J., and Harrison, S. C. (2000) Structure of PAK1 in an autoinhibited conformation reveals a multistage activation switch, *Cell 102*, 387−397.
12. Altman, S., and Kirsebom, L. (1999) Ribonuclease P, in *The RNA World* (Gesteland, R. F., Cech, T. R., and Atkins, J. F., Eds.) pp 351−380, CSH Press, Cold Spring Harbor, New York.
13. Frank, D. N., and Pace, N. R. (1998) Ribonuclease P: unity and diversity in a tRNA processing ribozyme, *Annu. Rev. Biochem. 67*, 153−180.
14. Kole, R., Baer, M. F., Stark, B. C., and Altman, S. (1980) *E. coli* RNAase P has a required RNA component, *Cell 19*, 881−887.
15. Talbot, S. J., and Altman, S. (1994) Gel retardation analysis of the interaction between C5 protein and M1 RNA in the formation of the ribonuclease P holoenzyme from *Escherichia coli*, *Biochemistry 33*, 1399−1405.
16. Westhof, E., Wesolowski, D., and Altman, S. (1996) Mapping in three dimensions of regions in a catalytic RNA protected from attack by an Fe(II)-EDTA reagent, *J. Mol. Biol. 258*, 600−613.
17. Tanaka, T., Ando, T., Haga, S., and Kikuchi, Y. (2004) Examining the bases of the J3/4 domain of *Escherichia coli* ribonuclease P, *Biosci. Biotechnol. Biochem. 68*, 1388−1392.
18. Peck-Miller, K. A., and Altman, S. (1991) Kinetics of the processing of the precursor to 4.5 S RNA, a naturally occurring substrate for RNase P from *Escherichia coli*, *J. Mol. Biol. 221*, 1−5.
19. Kurz, J. C., and Fierke, C. A. (2002) The affinity of magnesium binding sites in the *Bacillus subtilis* RNase P•pre-tRNA complex is enhanced by the protein subunit, *Biochemistry 41*, 9545−9558.
20. Kurz, J. C., Niranjanakumari, S., and Fierke, C. A. (1998) Protein component of *Bacillus subtilis* RNase P specifically enhances the affinity for precursor-tRNA^{Asp}, *Biochemistry 37*, 2393−2400.
21. Crary, S. M., Niranjanakumari, S., and Fierke, C. A. (1998) The protein component of *Bacillus subtilis* ribonuclease P increases catalytic efficiency by enhancing interactions with the 5′ leader sequence of pre-tRNA^{Asp}, *Biochemistry 37*, 9409−9416.
22. Niranjanakumari, S., Stams, T., Crary, S. M., Christianson, D. W., and Fierke, C. A. (1998) Protein component of the ribozyme ribonuclease P alters substrate recognition by directly contacting precursor tRNA, *Proc. Natl. Acad. Sci. U.S.A. 95*, 15212−15217.
23. Henkels, C. H., Kurz, J. C., Fierke, C. A., and Oas, T. G. (2001) Linked folding and anion binding of the *Bacillus subtilis* ribonuclease P protein, *Biochemistry 40*, 2777−2789.
24. Bolen, D. W., and Baskakov, I. V. (2001) The osmophobic effect: natural selection of a thermodynamic force in protein folding, *J. Mol. Biol. 310*, 955−963.
25. Makhatadze, G. I., and Privalov, P. L. (1995) Energetics of protein structure, *Adv. Protein Chem. 47*, 307−425.
26. Murphy, K. P., and Freire, E. (1992) Thermodynamics of structural stability and cooperative folding behavior in proteins, *Adv. Protein Chem. 43*, 313−361.
27. Gomez, J., Hilser, V. J., Xie, D., and Freire, E. (1995) The heat capacity of proteins, *Proteins 22*, 404−412.
28. Robertson, A. D., and Murphy, K. P. (1997) Protein structure and the energetics of protein stability, *Chem. Rev. 97*, 1251−1268.
29. Myers, J. K., Pace, C. N., and Scholtz, J. M. (1995) Denaturant *m* values and heat capacity changes: relation to changes in accessible surface areas of protein unfolding [published erratum appears in (1996) *Protein Sci. 5* (5), 981], *Protein Sci. 4*, 2138−2148.
30. Sturtevant, J. M. (1977) Heat capacity and entropy changes in processes involving proteins, *Proc. Natl. Acad. Sci. U.S.A. 74*, 2236−2240.
31. Pace, C. N., and Schmid, F. X. (1997) How to determine the molar absorbance coefficient of a protein, in *Protein Structure: A Practical Approach* (Creighton, T. E., Ed.) pp 253−259, Oxford University Press, Oxford, U.K.
32. Wang, A., and Bolen, D. W. (1997) A naturally occurring protective system in urea-rich cells: mechanism of osmolyte protection of proteins against urea denaturation, *Biochemistry 36*, 9101−9108.
33. Becktel, W. J., and Schellman, J. A. (1987) Protein stability curves, *Biopolymers 26*, 1859−1877.
34. Yancey, P. H., and Somero, G. N. (1980) Methylamine osmoregulatory solutes elasmobranch fishes counteract urea inhibition of enzymes, *J. Exp. Zool. 212*, 205−213.
35. Santoro, M. M., and Bolen, D. W. (1988) Unfolding free energy changes determined by the linear extrapolation method. 1. Unfolding of phenylmethanesulfonyl α-chymotrypsin using different denaturants, *Biochemistry 27*, 8063−8068.
36. Greene, R. F., Jr., and Pace, C. N. (1974) Urea and guanidine hydrochloride denaturation of ribonuclease, lysozyme, alpha-chymotrypsin, and beta-lactoglobulin, *J. Biol. Chem. 249*, 5388−5393.
37. Chen, B. L., and Schellman, J. A. (1989) Low-temperature unfolding of a mutant of phage T4 lysozyme. 1. Equilibrium studies, *Biochemistry 28*, 685−691.
38. Murphy, K. P. (1999) Predicting binding energetics from structure: looking beyond DeltaG degrees, *Med. Res. Rev. 19*, 333−339.
39. Murphy, K. P., Bhakuni, V., Xie, D., and Freire, E. (1992) Molecular basis of co-operativity in protein folding. III. Structural identification of cooperative folding units and folding intermediates, *J. Mol. Biol. 227*, 293−306.
40. Hilser, V. J., and Freire, E. (1996) Structure-based calculation of the equilibrium folding pathway of proteins. Correlation with hydrogen exchange protection factors, *J. Mol. Biol. 262*, 756−772.
41. Ferreon, J. C., Volk, D. E., Luxon, B. A., Gorenstein, D. G., and Hilser, V. J. (2003) Solution structure, dynamics, and thermody-

namics of the native state ensemble of the Sem-5 C-terminal SH3 domain, *Biochemistry 42*, 5582−5591.
42. Weinreb, P. H., Zhen, W., Poon, A. W., Conway, K. A., and Lansbury, J. P. T. (1996) NACP, a protein implicated in Alzheimer's disease and learning, is natively unfolded, *Biochemistry 35*, 13709−13715.
43. Deutschman, W. A., and Dahlquist, F. W. (2001) Thermodynamic basis for the increased thermostability of CheY from the hyperthermophile *Thermotoga maritima*, *Biochemistry 40*, 13107−13113.
44. Privalov, P. L. (1979) Stability of proteins: small globular proteins, *Adv. Protein Chem. 33*, 167−241.
45. Mendoza, C., Figueirido, F., and Tasayco, M. L. (2003) DSC studies of a family of natively disordered fragments from *Escherichia coli* thioredoxin: surface burial in intrinsic coils, *Biochemistry 42*, 3349−3358.
46. Georgescu, R. E., Garcia-Mira, M. M., Tasayco, M. L., and Sanchez-Ruiz, J. M. (2001) Heat capacity analysis of oxidized *Escherichia coli* thioredoxin fragments (1- -73, 74- -108) and their noncovalent complex. Evidence for the burial of apolar surface in protein unfolded states, *Eur. J. Biochem. 268*, 1477−1485.
47. Stams, T., Niranjanakumari, S., Fierke, C. A., and Christianson, D. W. (1998) Ribonuclease P protein structure: evolutionary origins in the translational apparatus, *Science 280*, 752−755.
48. Spitzfaden, C., Nicholson, N., Jones, J. J., Guth, S., Lehr, R., Prescott, C. D., Hegg, L. A., and Eggleston, D. S. (2000) The structure of ribonuclease P protein from *Staphylococcus aureus* reveals a unique binding site for single-stranded RNA, *J. Mol. Biol. 295*, 105−115.
49. Kazantsev, A. V., Krivenko, A. A., Harrington, D. J., Carter, R. J., Holbrook, S. R., Adams, P. D., and Pace, N. R. (2003) High-resolution structure of RNase P protein from *Thermotoga maritima*, *Proc. Natl. Acad. Sci. U.S.A. 100*, 7497−7502.
50. Cabrita, L. D., and Bottomley, S. P. (2004) How do proteins avoid becoming too stable? Biophysical studies into metastable proteins, *Eur. Biophys. J. 33*, 83−88.
51. Felitsky, D. J., and Record, M. T., Jr. (2004) Application of the local-bulk partitioning and competitive binding models to interpret preferential interactions of glycine betaine and urea with protein surface, *Biochemistry 43*, 9276−9288.
52. Truhlar, S. M., Cunningham, E. L., and Agard, D. A. (2004) The folding landscape of *Streptomyces griseus* protease B reveals the energetic costs and benefits associated with evolving kinetic stability, *Protein Sci. 13*, 381−390.
53. Baskakov, I., and Bolen, D. W. (1998) Forcing thermodynamically unfolded proteins to fold, *J Biol Chem 273*, 4831−4834.
54. Gursky, O. (1999) Probing the conformation of a human apolipoprotein C-1 by amino acid substitutions and trimethylamine-*N*-oxide, *Protein Sci. 8*, 2055−2064.
55. Schellman, J. A. (2003) Protein stability in mixed solvents: a balance of contact interaction and excluded volume, *Biophys. J. 85*, 108−125.
56. Felitsky, D. J., and Record, M. T., Jr. (2003) Thermal and urea-induced unfolding of the marginally stable lac repressor DNA-binding domain: a model system for analysis of solute effects on protein processes, *Biochemistry 42*, 2202−2217.
57. Ibarra-Molero, B., and Sanchez-Ruiz, J. M. (1996) A model-independent, nonlinear extrapolation procedure for the characterization of protein folding energetics from solvent-denaturation data, *Biochemistry 35*, 14689−14702.
58. Makhatadze, G. I., and Privalov, P. L. (1992) Protein interactions with urea and guanidinium chloride. A calorimetric study, *J. Mol. Biol. 226*, 491−505.
59. Niranjanakumari, S., Kurz, J. C., and Fierke, C. A. (1998) Expression, purification and characterization of the recombinant ribonuclease P protein component from *Bacillus subtilis*, *Nucleic Acids Res. 26*, 3090−3096.
60. Uversky, V. N., Gillespie, J. R., and Fink, A. L. (2000) Why are "natively unfolded" proteins unstructured under physiologic conditions?, *Proteins 41*, 415−427.
61. Santoro, M. M., Liu, Y., Khan, S. M., Hou, L. X., and Bolen, D. W. (1992) Increased thermal stability of proteins in the presence of naturally occurring osmolytes, *Biochemistry 31*, 5278−5283.
62. Kaushik, J. K., and Bhat, R. (1999) A mechanistic analysis of the increase in the thermal stability of proteins in aqueous carboxylic acid salt solutions, *Protein Sci. 8*, 222−233.
63. Kaushik, J. K., and Bhat, R. (2003) Why is trehalose an exceptional protein stabilizer? An analysis of the thermal stability of proteins in the presence of the compatible osmolyte trehalose, *J. Biol. Chem. 278*, 26458−26465.
64. Qu, Y., Bolen, C. L., and Bolen, D. W. (1998) Osmolyte-driven contraction of a random coil protein, *Proc. Natl. Acad. Sci. U.S.A. 95*, 9268−9273.
65. Day-Storms, J. J., Niranjanakumari, S., and Fierke, C. A. (2004) Ionic interactions between PRNA and P protein in *Bacillus subtilis* RNase P characterized using a magnetocapture-based assay, *RNA 10*, 1595−1608.
66. Myers, J. K., and Pace, C. N. (1996) Hydrogen bonding stabilizes globular proteins, *Biophys. J. 71*, 2033−2039.
67. Ladbury, J. E., Wright, J. G., Sturtevant, J. M., and Sigler, P. B. (1994) A thermodynamic study of the trp repressor-operator interaction, *J. Mol. Biol. 238*, 669−681.
68. Ha, J. H., Spolar, R. S., and Record, M. T., Jr. (1989) Role of the hydrophobic effect in stability of site-specific protein−DNA complexes, *J. Mol. Biol. 209*, 801−816.
69. Lee, B., and Richards, F. M. (1971) The interpretation of protein structures: estimation of static accessibility, *J. Mol. Biol. 55*, 379−400.
70. Mello, C. C., and Barrick, D. (2003) Measuring the stability of partly folded proteins using TMAO, *Protein Sci. 12*, 1522−1529.
71. Marcus, Y. (1994) A simple empirical model describing the thermodynamics of hydration of ions of widely varying charges, sizes, and shapes, *Biophys. Chem. 51*, 111−127.
72. Oda, M., Furukawa, K., Ogata, K., Sarai, A., and Nakamura, H. (1998) Thermodynamics of specific and non-specific DNA binding by the c-Myb DNA-binding domain, *J. Mol. Biol. 276*, 571−590.
73. Merabet, E., and Ackers, G. K. (1995) Calorimetric analysis of lambda cI repressor binding to DNA operator sites, *Biochemistry 34*, 8554−8563.
74. Lundback, T., Cairns, C., Gustafsson, J. A., Carlstedt-Duke, J., and Hard, T. (1993) Thermodynamics of the glucocorticoid receptor−DNA interaction: binding of wild-type GR DBD to different response elements, *Biochemistry 32*, 5074−5082.
75. Jin, L., Yang, J., and Carey, J. (1993) Thermodynamics of ligand binding to trp repressor, *Biochemistry 32*, 7302−7309.
76. Connelly, P. R., Thomson, J. A., Fitzgibbon, M. J., and Bruzzese, F. J. (1993) Probing hydration contributions to the thermodynamics of ligand binding by proteins. Enthalpy and heat capacity changes of tacrolimus and rapamycin binding to FK506 binding protein in D_2O and H_2O, *Biochemistry 32*, 5583−5590.
77. Lundback, T., Chang, J. F., Phillips, K., Luisi, B., and Ladbury, J. E. (2000) Characterization of sequence-specific DNA binding by the transcription factor Oct-1, *Biochemistry 39*, 7570−7579.
78. Spolar, R. S., and Record, M. T., Jr. (1994) Coupling of local folding to site-specific binding of proteins to DNA [see comments], *Science 263*, 777−784.
79. Gallagher, K., and Sharp, K. (1998) Electrostatic contributions to heat capacity changes of DNA-ligand binding, *Biophys. J. 75*, 769−776.
80. Morton, C. J., and Ladbury, J. E. (1996) Water-mediated protein−DNA interactions: the relationship of thermodynamics to structural detail, *Protein Sci. 5*, 2115−2118.
81. Cooper, A. (2005) Heat capacity effects in protein folding and ligand binding: a re-evaluation of the role of water in biomolecular thermodynamics, *Biophys. Chem. 115*, 89−97.
82. Lindorff-Larsen, K., Best, R. B., Depristo, M. A., Dobson, C. M., and Vendruscolo, M. (2005) Simultaneous determination of protein structure and dynamics, *Nature 433*, 128−132.
83. Bevington, P. R. (1969) *Data Reduction and Error Analysis for the Physical Sciences*, McGraw-Hill Book Company, New York.

BI0504613